Fabricating a reactive surface on the fibroin film by a room-temperature plasma jet array for biomolecule immobilization*

Chen Guang-Liang(陈光良)[a)†], Zheng Xu(郑 旭)[a)], Lü Guo-Hua(吕国华)[b)], Zhang Zhao-Xia(张朝霞)[a)], Sylvain Massey[c)], Wilson Smith[c)], Michael Tatoulian[c)], and Yang Si-Ze(杨思泽)[b)]

[a)] *Key Laboratory of Advanced Textile Materials and Manufacturing Technology of Ministry of Education, and Engineering Research Center for Eco-Dyeing & Finishing of Textiles, Zhejiang Sci-Tech University, Hangzhou* 310018, *China*

[b)] *Key Laboratory of Soft Matter Physics, Institute of Physics, Chinese Academy of Sciences, Beijing* 100190, *China*

[c)] *École Nationale Supérieure de Chimie de Paris–Chimie ParisTech, Laboratoire de Génie des Procédés Plasmas et Traitements de Surfaces, Université Pierre et Marie Curie, Paris* 75005, *France*

(Received 9 April 2012; revised manuscript received 21 June 2012)

A simple dielectric barrier discharge (DBD) jet array was designed with a liquid electrode and helium gas. The characteristics of the jet array discharge and the preliminary polymerization with acrylic acid (AA) monomer were presented. The plasma reactor can produce a cold jet array with a gas temperature lower than 315 K, using an applied discharge power between 6 W and 30 W ($V_{\rm dis} \times I_{\rm dis}$). A silk fibroin film (SFF) was modified using the jet array and AA monomer, and the treated SFF samples were characterized by atomic force microscopy (AFM), scanning electron microscopy (SEM), Fourier transform infrared spectroscopy (FTIR), and contact angle (CA). The deposition rate of the poly acrylic acid (PAA) was able to reach 300 nm/min, and the surface roughness and energy increased with the AA flow rate. The FTIR results indicate that the modified SFF had more carboxyl groups (–COOH) than the original SFF. This latter characteristic allowed the modified SFF to immobilize more quantities of antimicrobial peptide (AP, LL-37) which inhibited the Escherichia coli (E. Coli) effectively.

Keywords: plasma jet array, polymerizing modification, fibroin film, antimicrobial property

PACS: 52.75.Hn, 52.70.Kz, 52.80.Hc, 87.68.+z **DOI:** 10.1088/1674-1056/21/10/105201

1. Introduction

Recently, plasma-treated surfaces or plasma polymers as interfacial bonding layers for subsequent immobilization of molecules have elicited specific biological responses.[1−3] Normally, the surface modification is realized by vacuum non-equilibrium plasmas, which is well documented in the scientific literature.[4] However, disadvantages of this plasma technology include the requirement for an expensive vacuum pumping system, the restriction to the use of vacuum-compatible materials, and the difficulty to get continuous processing systems.[5] In recent years, much attention has been paid to atmospheric pressure glow discharge (APGD) sources, which have a similar ability to vacuum plasmas for getting homogeneous treatments and coatings. A typical APGD source, the low temperature plasma jet, has recently received significant attention due to its capability to treat three-dimensional surfaces,[6,7] deposit functional films,[8−10] and to sterilize bacteria.[11,12]

Although low temperature plasma jets have been studied intensively,[5−13] the study of jet polymerization has not attracted much attention, which limits our understanding in evaluation of the mechanisms and efficiency of these processes. Meanwhile, due to the various processing parameters (design configurations of the plasma reactors, different operation conditions, etc.), the importance of foregoing factors may be very different, especially with the addition of a reactive reagent in the plasma jet. Accordingly, it is necessary to explore the effects of reactive gases on the plasma jets and the characteristics of organic functional films deposited by the low temperature plasma

*Project supported by the National Natural Science Foundation of China (Grant No. 11175157), the Young Scientists Fund of the National Natural Science Foundation of China (Grant No. 11005151), the Natural Science Foundation of Zhejiang Province, China (Grant No. Y6100045), the Project for Zhejiang Provincial Key Innovation Team, China (Grant No. 2012R10038).

†Corresponding author. E-mail: glchen@zstu.edu.cn

© 2012 Chinese Physical Society and IOP Publishing Ltd

jet.

In the present work, a specially designed plasma jet array system with a highly conductive liquid electrode is reported, and an on-going pretreatment and modification of materials can be achieved in the same process. Moreover, the COOH-rich surface, which has many potential applications in the biomedical field,[14] is deposited by the jet polymerization of acrylic acid on SFF for immobilizing antimicrobial peptides.

2. Experimental

2.1. The experimental setup

Figure 1(a) shows the schematic diagram of the experimental apparatus. In the reactor, four quartz tubes with shaped nozzles (inner diameter: 6 mm, outer diameter: 8 mm, and outlet diameter: 4 mm) were the dielectric layer fixed in an organic glass tank by Teflon fittings. Copper tubes centered in the quartz tubes were the first electrode, and a potassium chloride (KCl) solution in the tank acted as the other electrode. The conductive liquid electrode was directly in contact with the dielectric layer, so the system could generate a more uniform plasma. Meanwhile, the liquid electrode also served as a coolant for the discharge system and allowed the setup to run longer. Both electrodes were connected to a commercial AC power supply (SP-2000C, Nanjing, Suman, China) with a maximum peak voltage of 30 kV and an adjustable frequency from 10 kHz to 30 kHz. The helium velocity and reactive gases were controlled by a rotameter and a mass flowmeter, respectively. The oxygen gas and the vaporized acrylic acid (water bath temperature: 60 °C) were carried to the jet center by tube 1 and tubes 1, 2, 3. The first jet which carried oxygen was used for a pretreatment (grafting polar groups) of the fiber surface. This pretreatment also increased the hydrophilic properties of the fiber, and greatly increased the adhesion strength between the polymer and the fiber. It should be noted that the prepared SFF was fixed on the belt for plasma treatment. Figure 1(b) shows the helium plasma jet array generated at a helium velocity of 4 m/s and an applied power of 12 W. The processing parameters are presented in Table 1, and the other parameters were kept constant when one parameter changed.

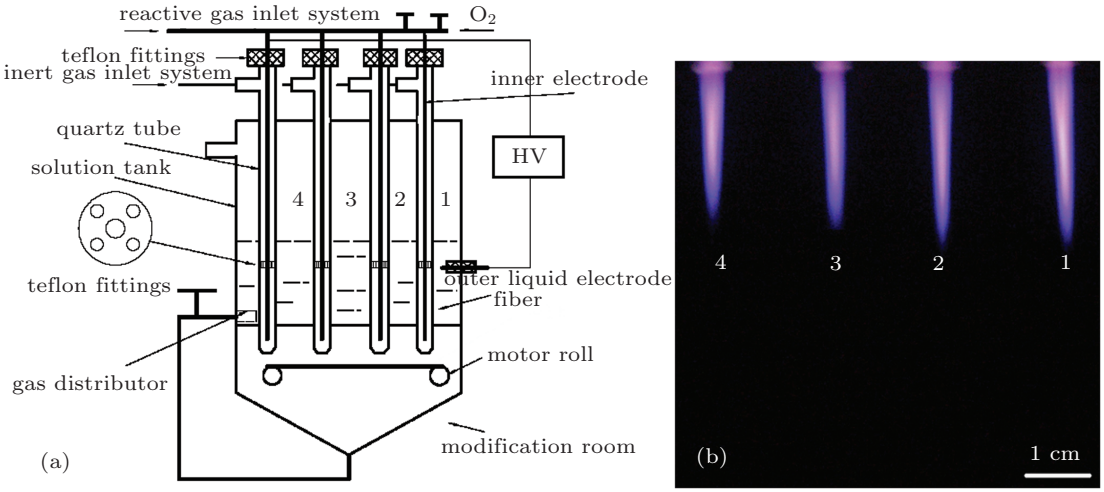


Fig. 1. (colour online) (a) Schematic diagram of the experimental setup. (b) Picture of the low-temperature plasma plume array with an He rate of 7 L/min and a power of 12 W.

Table 1. Polymerizing parameters of the APDG jet array for SFF modification.

Parameter values	
Applied power/W	12–30
He velocity/L·min^{-1}	7–10
O_2 velocity/L·min^{-1}	3.5
AA flow rate/sccm	5–20
Depositing time/min	2–10
Jet-substrate distance/cm	0.5

2.2. The plasma diagnostics

Using a digital oscilloscope (Tektronix, TDS1012B), the applied potential voltage between the electrodes was monitored with an HV probe (Tektronix, P6015A). The plasma jet and circuit currents were measured using a current probe (Tektronix, P6021) by following the same method used in a previous study.[13] An infrared thermometer

(Fluke USA, Fluke 66) was used to measure the plasma gas temperature. Although it is difficult to directly measure the temperature of the transparent plasma gas by using the infrared thermometer, we overcame this obstacle by using an insulating epoxy plate (2 cm×1 cm×0.15 cm, $L \times W \times T$) and kept it in contact with the plasma jet. Then, we measured the temperature at the contact point with the infrared thermometer, giving us an indication of the plasma gas temperature. The reactive species present in the plasma were identified with a typical UV-visible emission spectrometer (American Stellarnet, EPP-2000C).

2.3. The functional film analysis

The static contact angle (CA) of the films was characterized using a Kruss Drop Shape Analysis System (Germany Kruss GmbH, DSA10), and a drop of distilled water with a volume of 5 μL was placed on the SFF surface using a syringe with a 22-gauge needle. The contact angles were the average of three measuring samples fabricated with the same plasma parameters, and the standard deviation was 1°. In order to investigate the AA polymer stability on the SFF, the samples were washed with water for 5 h and dried in an oven for 3 h. The change in the CA of the washed samples were used to determine the AA polymer stability. The roughness of the functional films was estimated by an atomic force microscope (AFM) (XE-100E, PSIA, Korea) in air under ambient conditions, and the characterization was made in a non-contact mode with an NSC-15/Al probe. The chemical structure of the AA polymer was analyzed by a Fourier transform infrared spectroscopy (FTIR) (Thermo Electron Corp., USA) instrument in the range of 400 cm^{-1}–4000 cm^{-1} with a resolution of 4 cm^{-1}. The thickness of the PAA was determined by measuring the cross-section of the as-deposited films with a field mission scanning electron microscope (SEM) (Hitachi, S4800).

2.4. The antimicrobial activity of modified SFF with immobilized antimicrobial peptide

The activation of the modified SFF (with a polymerized AA layer on the SFF surface), and the immobilization of the antimicrobial peptide LL-37 which has a sequence of H-LLGAPPALSLGLIGLGPLAIVGAILAPLAALVPATGS-OH (purchased from GL Biochem. Shanghai Ltd., China), was carried out following a similar procedure described by Bai *et al.*[14] The immobilizing process of LL-37 peptide on the modified SFF surface is depicted in Fig. 2. The cultured E. coli bacteria, which is the main infection species used in biotechnology, was used to probe the antimicrobial activity of the SFF immobilized LL-37.

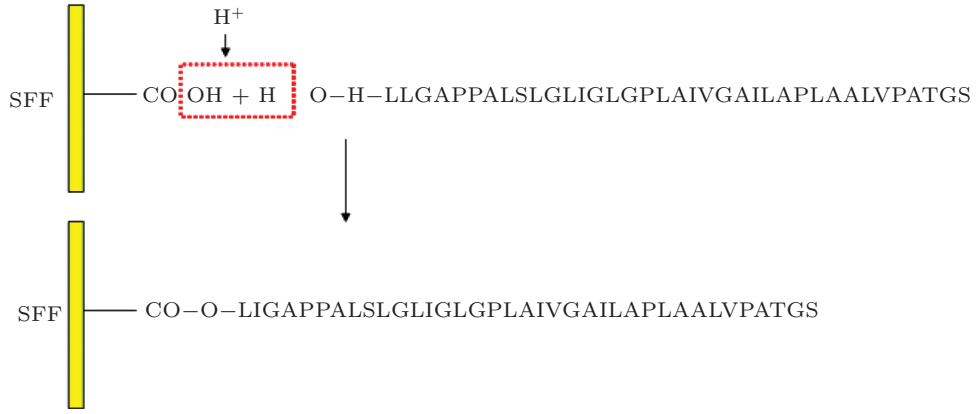


Fig. 2. The immobilizing process of LL-37 on the modified SFF.

3. Results and discussion

3.1. The preliminary discharging characterization of the jet array

In order to investigate the electric current carried by the plasma jets, the current of the second jet in the plasma device was measured with a Tektronix current probe. The jet diameter taken 1 cm away from the jet outlet was only 3 mm, which was smaller than the probe jaw diameter (4 mm). Therefore, it allowed us to measure the jet current by letting the plasma jet go through the probe jaw. Figure 3 shows the effects of the input voltage on the jet current. When the dis-

charge voltage was 1.4 kV (see Fig. 3(a)), the jet current was only 5 mA. When the voltage was increased from 2.1 kV to 2.3 kV, the jet current increased from 47 mA to 75 mA (see Figs. 3(b) and 3(c)). The results showed that the discharge voltage had a significant effect on the jet current, and a higher discharge voltage may increase the density of the reactive species which is effective for improving the film deposition rate. Figure 4 shows the influence of the AA present in the plasma on the jet current. Compared with the results of Fig. 3(b), the inert gas flow rate also affected the jet current, because the jet current increased to nearly 60 mA at a lower discharge voltage (1.7 kV) when the He flow velocity increased from 4 m/s to 6 m/s. In addition, the jet current decreased significantly when the monomer was carried to the jet center. The reason for this may be that the AA gas quenched many electrons which were generated in the plasma jet.

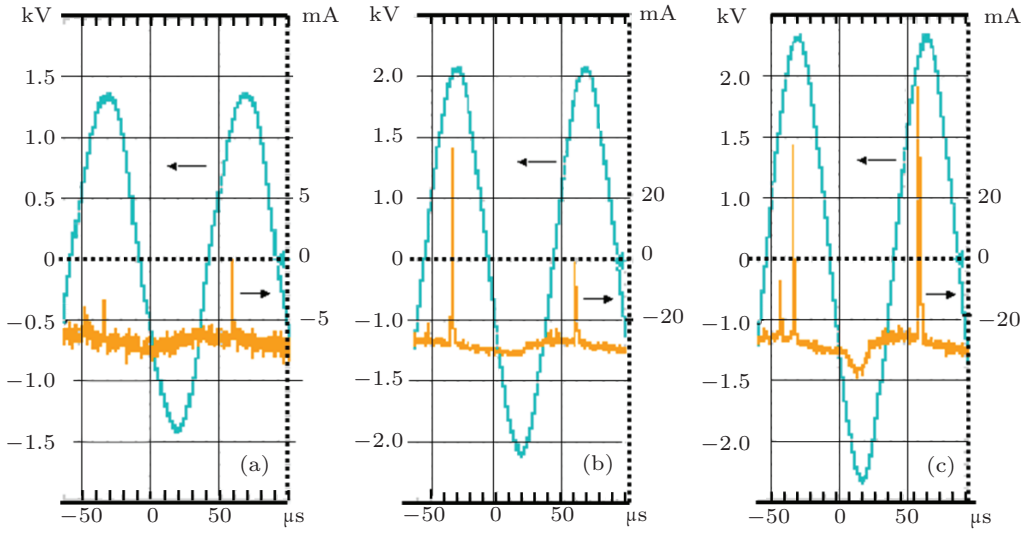


Fig. 3. (colour online) Time traces of total applied voltage and tube 2 jet current with a discharge frequency of 10.3 kHz and an He velocity of 10 L/min: (a) 1.4 kV, (b) 2.1 kV, (c) 2.3 kV.

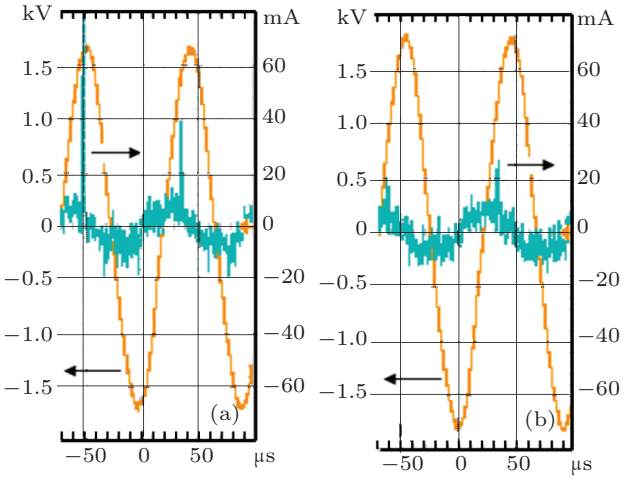


Fig. 4. (colour online) Effect of the AA monomer on the jet current: (a) without AA, (b) with 5 sccm of AA monomer. The parameters for the plasma are an applied voltage of 1.7 kV and an He flow rate of 7 L/min. The distance between the outlet and the measuring point was 1 cm.

Figure 5(a) presents the relationship between the liquid height in the tank and the applied power. With the same He gas velocity (7 L/min) and the same applied voltage (4.5 kV), the outer liquid electrode height greatly affected the power consumption. The inset of Fig. 5(a) displays the equivalent circuit of the discharge system according to previous reports.[15] As the discharge area was enlarged, the resistance of the outer electrode increased, and the outer electrode consumes a higher input power. Meanwhile, the discharge area increased, and the power distributed on each discharge unit decreased. As a result, more discharge channels were quenched, and the discharge current decreased at the same input power. Therefore, the optimized liquid height should be studied in this system similarly to the previous study[16] which was used in the degradation of an azo dye solution. Gas temperature is another important parameter in the modification of materials. The vibrational temperature of the plasma jet (data trend 2 in Fig. 5(b)) was determined by the simulated spectra of the $C^3\Pi_u$–$B^3\Pi_g$ ($\Delta v = -2$) band transition of nitrogen. The vibrational temperature was not higher than 306 K when the applied power was lower than 30 W. In order to calibrate the simulated temperature, an infrared ther-

mometer was used to measure the plasma gas temperature (data trend 1 in Fig. 5(b)). The results were taken using a similar procedure explained in our previous work.[17] It is observed that data trend 1 are lower than data trend 2 under the same discharge conditions. This means that the rotational temperature obtained by the spectrum simulation is higher than the actual plasma gas temperature because of the jet thermal energy accumulated on the contact point where the temperature was measured with the infrared thermometer. However, the obtained values are nearly at room temperature, and the use of a low temperature is very important for the modification of organic materials and monomer polymerization in order to preserve the materials.

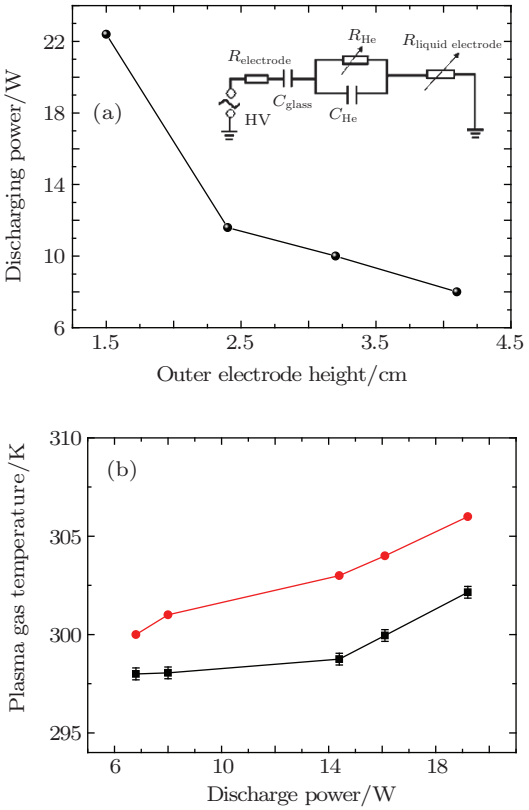


Fig. 5. (colour online) (a) Relationship between the outside electrode height and the applied power, with an He flow rate of 10 L/min and a discharge voltage of 5 kV. (b) Plasma gas temperature of the jet array. Data line 1 was measured by an infrared thermometer and data line 2 was simulated by an OES method.

3.2. Coating PAA on the SFF surface by the plasma jet array

Figure 6 shows the morphology of an SFF modified by the APGD jet array and an AA monomer. The original SFF spun on the silicon substrate is very smooth and the surface roughness is only 1.3 nm (see Fig. 6(a)). When the SFF was pretreated by the He and O_2 plasma which was generated in jet 1, the surface roughness of the SFF changed from 1.3 nm to 2.3 nm. In addition, reactive polar groups (e.g. –OH) may be grafted on the SFF for oxygen presented in the He plasma. Although the change in roughness of

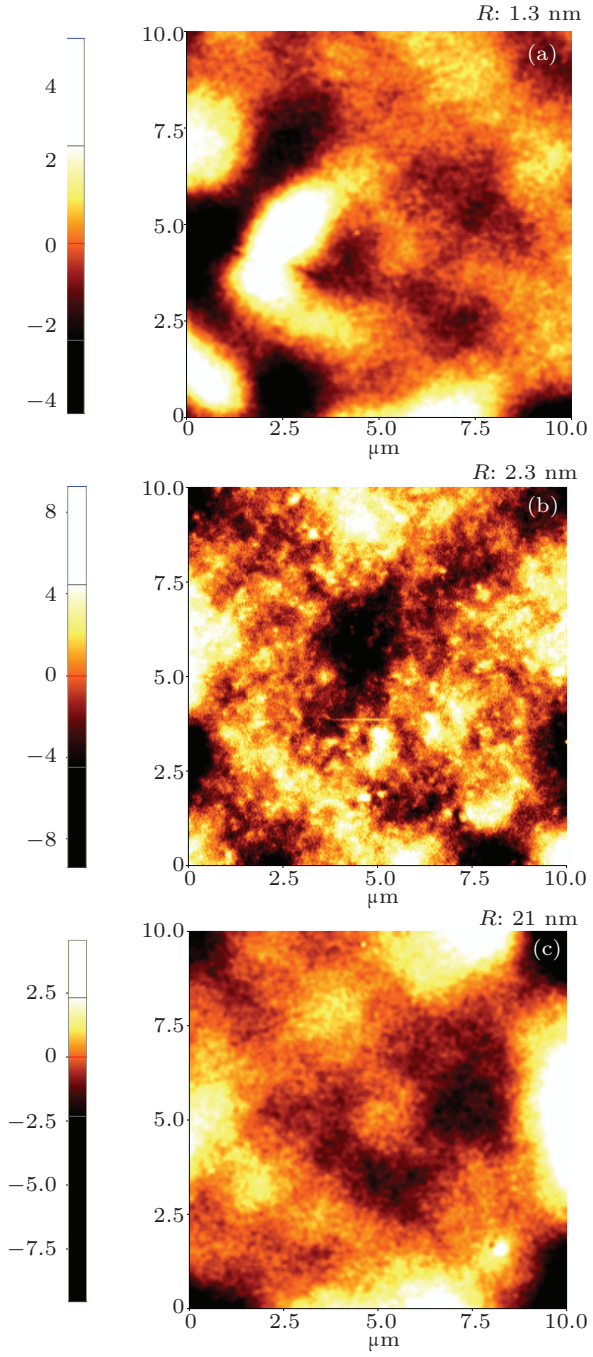


Fig. 6. (colour online) The AFM morphology of SFF treated by He plasma with oxygen and AA monomer. The He velocity and discharging power is 10 L/min and 20 W, respectively. (a) The original SFF, (b) the pretreated SFF with oxygen flow rate of 10 sccm, (c) the modified SFF with a monomer flow rate of 12 sccm.

SFF is not obvious, some micro-pits appeared on the treated SFF surface (see Fig. 6(b)).The introduced polar groups and the micro-pits on the SFF can improve the bonding intensity between the deposited polymer and the SFF substrate. Compared with the conventional phenomena generated in the process of plasma etching,[18] the micro-arcings were generated between the plasma jet and the SFF surface when AA occurred in the jet, which could be responsible for ablating many micro-pits on the SFF surface. With the same discharge power (20 W) and He velocity (10 L/min) as the pretreatment process, the surface roughness increased from 2.3 nm to 21 nm when the AA monomer was added in tubes 2, 3, and 4 (see Fig. 6(c)).

Figure 7(a) presents the influence of the input power on the PAA deposition rate and the contact angle. An increase in discharge power results in an increase of the plasma density accordingly as well as the ionization of acrylic acid molecules. Consequently, the PAA deposition rate increased as the input power increased. Normally, there are three regions, which are the monomer sufficient region, competition region, and monomer deficient region, in the deposition process of polymer.[19] The trend of the deposition rate with discharge power indicated that a discharge power of 12 W–30 W was still in the monomer sufficient region for the APGD jet array, and a higher discharge power should be used for fabricating a thicker PAA film. Meanwhile, the hydrophilicity of the SFF was increased as the water CA passed from 71° to 16° with the thicker PAA film coated on the SFF surface, revealing that the plasma treatment has introduced reactive polar groups on the SFF surface or increased the surface roughness of SFF (see Fig. 5) which can increase the surface energy according to Wenzel's equation.[19] Figure 7(b) shows the effect of the AA flow rate on the PAA depositing rate and the surface roughness. An increase in the monomer flow rate which manifests the deposition process in the monomer sufficient region[1] will result in an increase of polymerizing precursor. Therefore, a nearly linear relationship between the deposition rate of PAA and the AA flow rate was found when the discharge power of the jet array was 30 W. Meanwhile, the surface roughness of the PAA increased greatly when the AA flow rate changed from 5 sccm to 20 sccm. The increased monomer flow rate can keep the depositing system working in the monomer sufficient region (power deficient), which favors the formation of reactive groups and the deposition rate of the polymer.[20] However, the film homogeneity and stability may decrease because bigger particles of PAA were formed in the PAA film (see the inset of Fig. 7(b)), and the defect will influence the stability of the PAA film in a solution for bio-molecule immobilization.

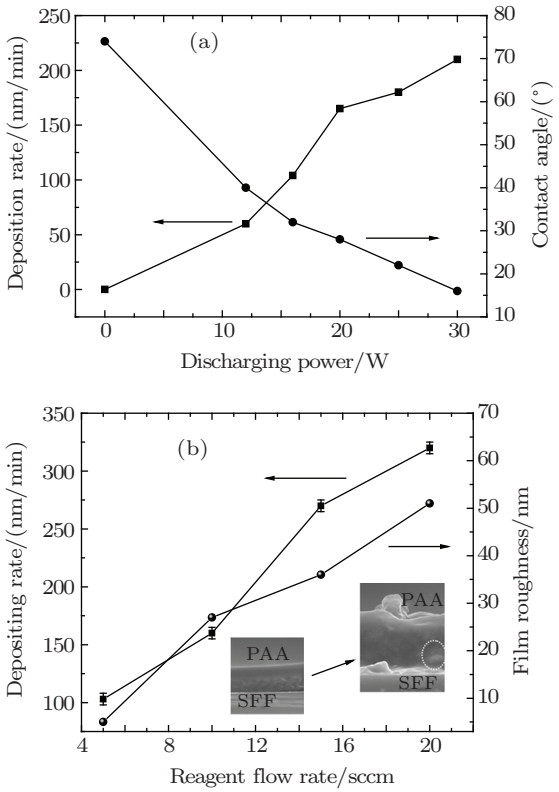


Fig. 7. (a) The effect of discharge power on the PAA deposition rate and the water contact angle with a monomer flow rate of 12 sccm and an He velocity of 10 L/min. (b) The influence of the monomer flow rate on the PAA deposition rate and surface roughness with a discharge power of 30 W and an He velocity of 10 L/min. The insets are the surface changes of SFF coated by PAA with different discharge powers.

Because the stability of the polymerized film is essential for application in bio-molecular fields, the solubility of poly acrylic acid in water was also investigated. Figure 8(a) shows the relationship between the contact angle and the washing time of the modified SFF in water. It can be found that the contact angle varied somewhat when the washing time was 5 h or less. This result is consistent with the result obtained by Morent *et al.*[21] Furthermore, using a higher power in a polymerizing process is good for forming a cross-linking structure on the AA polymer surface, since the cross-linking property greatly improves the polymer stability in solution. Figure 8(b) illustrates the FTIR spectra of the PAA polymer coated on the SFF surface with different discharging powers. In order to decrease the SFF effect on the analysis of the PAA

structure, the SFF acted as the background for the FTIR measurement of the PAA samples. The main bands of the PAA film were observed at 3300 cm^{-1} for O–H stretching, 2930 cm^{-1} for $–CH_x$ symmetrical stretching, and 1660 cm^{-1} for C=O stretching. The figure also shows that the main peak at 3100 cm^{-1}–3700 cm^{-1} for COOH/R stretching became stronger when the discharge power increased. However, most work in low pressure systems show that the power deficient region is good to form less extensive fragmentation of monomers and retains a substantial density of the reactive groups, such as carboxyls.[1] The difference in the trend between the high and low pressure plasmas indicates that: 1) the power we used is 'power deficient' in comparison with the monomer flow rate; 2) the atmospheric glow plasma perhaps does not follow the same law as the low pressure plasma. Certainly, these questions need to be confirmed in future work.

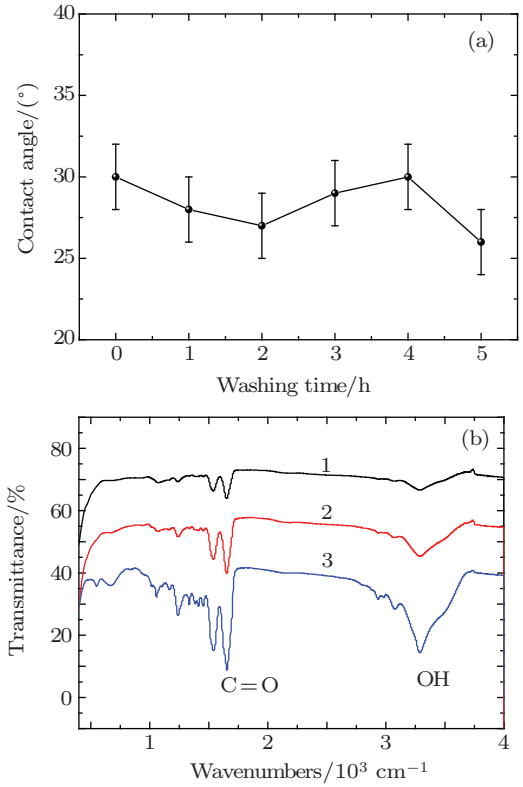


Fig. 8. (colour online) (a) PAA polymer stability under washing with water. (b) FTIR spectra of PAA coated on the SFF surface with a monomer flow rate of 12 sccm and an He velocity of 10 L/min. Curves 1, 2, and 3 are for 10 W, 20 W, and 30 W, respectively.

3.3. The antimicrobial property of modified SFF

Figure 9 presents the antimicrobial characteristics of the modified SFF with respect to the E. coli bacteria. The original SFF did not inhibit E. coli propagation, and the cultured bacteria covered the whole area around the SFF (see Fig. 9(a)). When using the original SFF with the immobilized antimicrobial peptide LL-37, an inhibiting ring was formed (see Fig. 9(b)). However, some E. coli bacteria were still observed in the ring. This may be due to the fact that the density of carboxyl groups on the original SFF was very low, and the amount of immobilized LL-37 was not great enough to kill the E. coli bacteria entirely. Therefore, the original SFF is not suitable to be used directly as a reactive surface for bio-molecule immobilization and cell colonization. In contrast to the original SFF, most of the E. coil bacteria in the inhibiting ring were killed when the LL-37 was immobilized on the SFF surface coated with AA polymer (Fig. 9(c)). In addition, the success in immobilizing a higher concentration of LL-37 on the modified SFF proved that the solubility of the AA polymer coated on the SFF was very low and a cross-linking structure may be formed in the AA polymer.

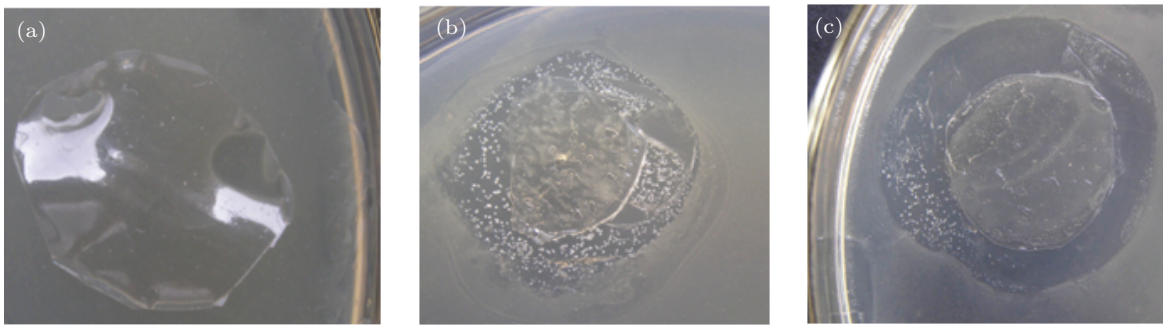


Fig. 9. (colour online) Inhibiting characteristics of a modified SFF with immobilized AP to the Escherichia coli. (a) Original SFF, (b) SFF with immobilized LL-37, (c) modified SFF and immobilized LL-37.

4. Conclusion

In summary, a low-temperature plasma jet array using a liquid electrode is studied. It was found that the chemical monomer and the discharge voltage significantly affected the plasma jet current. The deposition rate of the poly AA by the He plasma jet array was about 300 nm/min, which is primarily useful for the surface modification of many functional materials. The pure He jet had no effect on the materials in a short time, but was functionalized when the active gases and chemical reagents were added to the plasma jet array. In addition, a high density of carboxyl groups can be grafted on the SFF surface by the plasma jet array using an AA monomer. With this technique, a larger quantity of antimicrobial peptides can be immobilized on the SFF surface. Therefore, the plasma jet array has promising potential applications in materials modification as well as in the biomedical materials field.

Acknowledgement

The authors are grateful to professor Lu Xin-Pei for the help with the spectra simulation.

References

[1] Siow K S, Britcher L, Kumar S and Griesser H J 2006 *Plasma Process. Polym.* **3** 392

[2] Chen G L, Zhou M Y, Zhang Z X, Lü G H, Massey S, Smith W and Tatoulian M 2011 *Plasma Process. Polym.* **8** 701

[3] Xiong Z, Lu X, Cao Y, Ning Q, Ostrikov K, Lu Y, Zhou X and Liu J 2011 *Appl. Phys. Lett.* **99** 253703

[4] Sarra-Bournet C, Turgeon S, Mantovani D and Larochae G 2006 *Plasma Process. Polym.* **3** 506

[5] Tatoulian M, Arefi-khonsari and Borra J P 2007 *Plasma Process. Polym.* **4** 360

[6] Cao Z, Walsh J L and Kong M G 2009 *Appl. Phys. Lett.* **94** 021501

[7] Chen G L, Chen S H, Chen W X and Yang S Z 2008 *Chin. Phys.* B **17** 4568

[8] Lommatzsch U and Ihde J 2009 *Plasma Process. Polym.* **6** 642

[9] Raballand V, Benedikt J and von Keudell A 2008 *Appl. Phys. Lett.* **92** 091502

[10] Anthony P, Herbert F, O'Neill L and Jaroszyńska-Wolińska J 2009 *Chem. Mater.* **21** 4401

[11] Zhang X H, Huang J, Liu X D, Peng L, Guo L H, Lü G H, Chen W, Feng K C and Yang S Z 2009 *J. Appl. Phys.* **105** 063302

[12] Brian L S, Biswa N G and Kunihide T 2008 *Appl. Phys. Lett.* **92** 151503

[13] Li X C, Jia P Y, Yuan N and Chang Y Y 2012 *Chin. Phys.* B **21** 045204

[14] Bai L Q, Zhu L J, Min S J, Liu L, Cai Y R and Yao J M 2008 *Appl. Surf. Sci.* **254** 2988

[15] Dong L F, Mao Z G, Yin Z Q and Ran J X 2004 *Appl. Phys. Lett.* **84** 5142

[16] Chen G L, Zhou M Y, Chen S H and Chen W X 2009 *Journal of Hazardous Materials* **172** 786

[17] Chen G L, Chen S H, Chen W X and Yang S Z 2008 *Surf. Coat. Technol.* **202** 4741

[18] Stopford J, Allen D, Aldrian O, Morshed M, Wittge J, Danilewsky A N and McNally P J 2011 *Microelectronic Engineering* **88** 64

[19] Inagaki N 1996 *Plasma Surface Modification and Plasma Polymerization* (Basel: Technomic, Lancaster)

[20] Muller M and Oehr C 1999 *Surf. Coat. Technol.* **116** 802

[21] Morent R, Geyter N, Trentesaux M, Gengembre L, Dubruel P, Leys C and Payen E 2010 *Appl. Surf. Sci.* **257** 372